Options for Line-of-Sight Signal Transmission of the Recycler Stochastic Cooling Systems

Gerald Jackson
Fermi National Accelerator Laboratory, P.O. Box 500, Batavia IL, 60510

October 27, 1997

1. Introduction

The Recycler ring is a storage ring designed to accumulate and cooling a particle beam composed of antiprotons. Whereas the eventual method of emittance reduction will be electron cooling, the initial method will be stochastic cooling. It is therefore important to understand how implement horizontal, vertical, and momentum cooling systems.

It turns out that one of the two major normal arcs is necessary in order to for a pickup electrode derived beam signal to cut a chord and meet the beam at the kicker electrodes. Because of the existence of obstacles on the MI-50 side of the Reycler, the MI-20 side was chosen.

2. Antiproton Considerations

For the horizontal and vertical cooling systems, the phase advance between the pickup and kicker must be an odd multiple of 90°. Since the phase advance per cell in the Recycler is 85.387° horizontally and 79.220° vertically, over approximately 35 half cells of distance the differential phase advance can be quite large. As it turns out, if the number of cells between the horizontal (vertical) pickup and kicker is 18 (17) cells, then the number of betatron oscillations between them is 4.27 (3.74). This corresponds to a horizontal (vertical) net phase advance of 97° (94°), more than close enough to obtain optimal cooling rates.

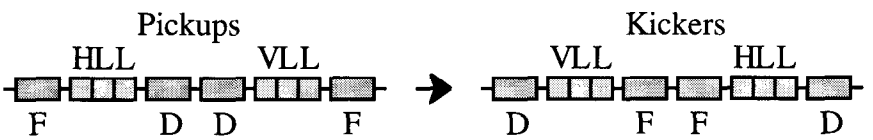

Figure 2.1: Geometry which keeps the 6 pickup tanks (an 6 kicker tanks) packed closely together while providing for 1 cell differential in relative horizontal and vertical phase advance. The darkly shaded objects are gradient magnets.

Figure 2.1 shows the optimum packing scenario for placement of the horizontal, vertical, and momentum pickup and kicker tanks to achieve the relative betatron phase advance between the horizontal and vertical systems. There is 163.6 in. between the beam position monitors in the straight sections between pairs of normal arc gradient magnets. The pickup tanks are 54 in. long each. Therefore, three tanks just fit in each half cell. If the horizontal pickup is placed just downstream (antiproton direction) of a focussing gradient magnet, then since two tanks fit between gradient magnets, the longitudinal pickup tank is just downstream of the defocussing gradient magnets. At the kicker end the ordering of the vertical and horizontal kicker tanks are reversed about a pair of focussing gradient magnets.

The length of a normal arc cell is 34.575 m. The kinetic energy of the antiprotons is 8.000 GeV. Table 2.1 summarizes the kinematics and timing of the antiprotons for the

horizontal and vertical systems. The momentum systems are identical since they are linked geometrically to the tranverse systems in this model calculation.

Table 2.1: Kinematic and timing considerations for the horizontal and vertical stochastic cooling systems under a model geometry in which all tanks are within the normal arc cells around MI-20 in the Reycler.

Parameter	Value
Antiproton Kinetic Energy (GeV)	8.000
Antiproton Mass (GeV)	0.93827231
Antiproton Total Energy (GeV)	8.938
Antiproton Momentum (GeV/c)	8.889
Antiproton Relativistic Energy	9.52631
Antiproton Relativistic Velocity	0.994475
Speed of Light in Vacuum (m/ns)	0.299792458
Length of a Normal Recycler Arc (m)	34.5752
Distance between Horizontal Tanks (cells)	18
Distance between Vertical Tanks (cells)	17
Distance between Horizontal Tanks (m)	622.386
Distance between Vertical Tanks (m)	587.778
Distance between Horizontal Tanks (ns)	2087.6
Distance between Vertical Tanks (ns)	1971.5

3. Lattice Considerations

This region of the Recycler lattice is regular, with only one type of lattice cell type. On the other hand, there are some injection devices which will limit the flexibility one may otherwise have placing tanks.

The most important limitation is the existence of the MI-22 transfer line and Lambertson. Aiming toward MI-30, the transfer line is terminated at the Lambertson just downstream of the gradient magnets over MIQ214 (between MIQ214 and MIQ215). Therefore, the most downstream position available for placement of a stochastic cooling pickup is the straight section between MIQ213 and MIQ214). The most upstream limit of the normal arc cell section is MIQ108, for a total of 17.5 cells. Since 18 cells are required in the horizontal plane, the horizontal kicker tank must reside in the first dispersion suppression cell. The length of available straight section in a dispersion suppression half cell is 102.1 in., too small for even two tanks. Figure 3.1 contains a sketch of the geometry proposed for this implementation of stochastic cooling.

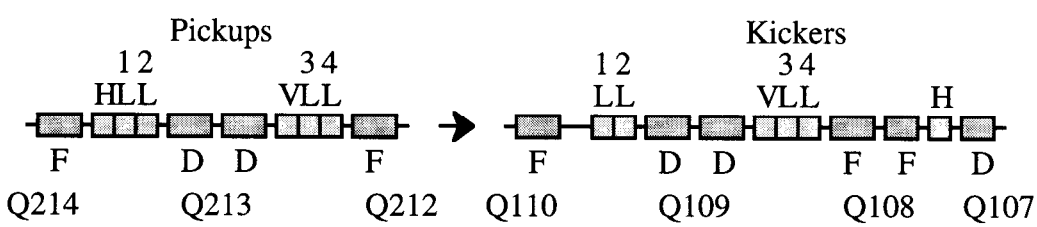

Figure 3.1: Geometry required to implement stochastic cooling in the Recycler ring. While the pickup side is identical to the model concept in section 2, the horizontal kicker is now in a dispersion suppression cell.

The one big disadvantage of this geometry is that the horizontal pickup is only 11.6 m away from the injection Lambertson. This means that the horizontal pickup must have the full horizontal aperture of 3.8", which desensitizes the system dramatically. One option is to use a 4 electrode geometry for the horizontal pickup, which has no horizontal aperture restriction and a higher horizontal sensitivity.

Table 3.1: Downstream longitudinal coordinates of the pickup and kicker tanks in the Recycler. These numbers were lifted from the mechanical drawings generated by Terry Anderson for the vacuum system.

Parameter	Pickup	Kicker	Distance
Horizontal Coordinate (ft.)	6601.152	8637.519	2036.367
Longitudinal #1 Coordinate (ft.)	6605.652	8534.120	1928.468
Longitudinal #2 Coordinate (ft.)	6610.152	8538.620	1928.468
Vertical Coordinate (ft.)	6657.872	8586.340	1928.468
Longitudinal #3 Coordinate (ft.)	6662.372	8590.840	1928.468
Longitudinal #4 Coordinate (ft.)	6666.872	8595.340	1928.468

From mechanical drawings of the Recycler ring the beamline distance coordinates of the (proton direction) downstream end of each pickup and kicker tank can be determined. The data is presented in table 3.1 Plugging this information into the data shown in table 2.1, enough information exists to calculate the distance between the pickup and kicker tanks of each of the four stochastic cooling systems. These distances are shown in table 3.2.

Table 3.2: Timing considerations for the stochastic cooling systems for the actual Recycler geometry.

Parameter	Value
Feet per Meter Conversion	3.280839895
Horizontal Distance (m)	620.685
Longitudinal #1 Distance (m)	587.797
Longitudinal #2 Distance (m)	587.797
Vertical Distance (m)	587.797
Longitudinal #3 Distance (m)	587.797
Longitudinal #4 Distance (m)	587.797
Horizontal Distance (ns)	2082
Longitudinal #1 Distance (ns)	1972
Longitudinal #2 Distance (ns)	1972
Vertical Distance (ns)	1972
Longitudinal #3 Distance (ns)	1972
Longitudinal #4 Distance (ns)	1972

4. Signal Transmission Geometry: Worst-Case Scenario

Because the shortest distance is usually via a straight line, and because of surface obstacles which limit the placement of the trench into which the vacuum pipe transmitting the laser beams is placed, the vacuum pipe and accompanying enclosures and conduits fall on the chord between MIQ213 and MIQ109. The site coordinates for these quadrupoles are known and listed in table 4.1. Note that the typical grade elevation in this section of the ring is approximately 740'.

Table 4.1: Site coordinates for the Main Injector quadrupole centers which determine the signal transmission path for the Recycler stochastic cooling systems.

Parameter	MIQ213	MIQ109
Project Coordinate X (ft.)	98960.55221	99356.30336
Project Coordinate Y (ft.)	95391.83193	97117.96262
Nominal Recycler Elevation (ft.)	720.5	720.5
Longitudinal Distance (ft.)	6636.000	8565.000

Table 4.2: Calculation of the relative angles between the Recycler ring tangent and the chord at the two quadrupoles.

Parameter	MIQ213	MIQ109
Chord Angle (deg.)	257.1	257.1
Recycler Tangent Angle (deg.)	297.7	36.5
Relative Angle (deg.)	40.6	40.6
Cosine of the Relative Angle	0.759	0.759
Sine of the Relative Angle	0.651	0.651

The angle between this chord and the ring itself is calculated in table 4.2. The definition of angle is

$$\theta = \arctan\left(\frac{\Delta Y}{\Delta X}\right) \quad . \qquad (4.1)$$

The minimum distance between the closest tunnel wall and the location of the laser launch cave is 26' in order for the enclosure to not be a controlled radiation area. Therefore, the minimum distance between the tunnel and cave along the chord is 40' = 12 m. This also means that the width of the berm above the tunnel is elongated by approximately 40% to about 70'. In figure 4.1 a sketch of the tunnel/chord configuration on either side of the chord is sketched. A 3' high pipe 12-18" in diameter is placed on top of the tunnel in case electronics needs to be hidden from radiation showers.

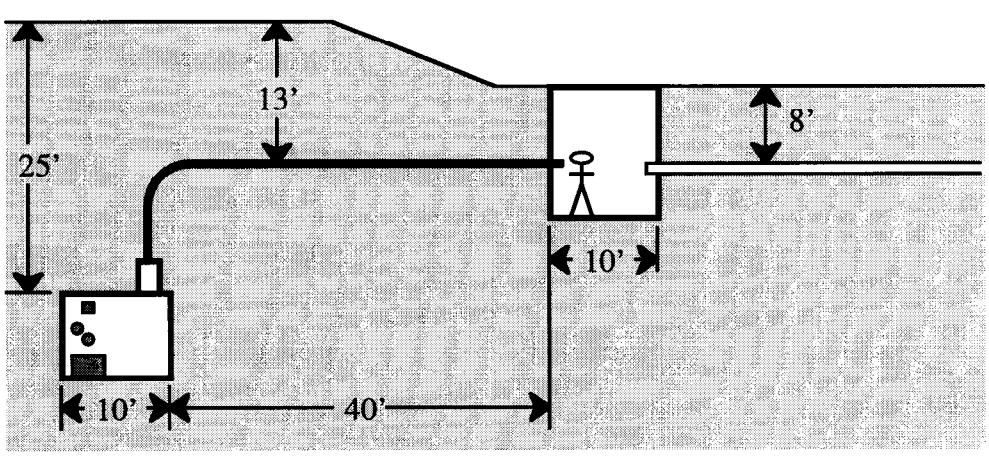

Figure 4.1: Sketch of the geometry used in signal delay calculations presented in this paper. This is the elevation view along the length of the chord between MIQ213 and MIQ109.

The assumption used in this paper is that all signal parthways between pickup and kicer tanks are either vertical, along the chord, or along the beamline. This is a conservative assumption, since there are ways to "cut corners" if another class of assumptions is made. The distances along the chord are summarized in table 4.3. The distances for each cooling system along the beamline are listed in table 4.4, where the distance assumes that the transmission cable extends from the Main Injector quadrupole to the far side of the pickup or kicker tank in question.

Table 4.3: Length of the signal pathways along the chord between MIQ213 and MIQ109.

Parameter	Value
Total Length of the Chord (ft.)	1771
Length of the Laser Telescope (ft.)	1657
Horizontal Cable Length (ft.)	114
Vertical Cable Length (ft.)	26

Table 4.4: Distance between the relavant quadrupole on the chord and the far side of the pickup or kicker tank.

Parameter	Pickup	Kicker
Horizontal Distance (ft.)	34.85	77.02
Longitudinal #1 Distance (ft.)	30.35	30.88
Longitudinal #2 Distance (ft.)	25.85	26.38
Vertical Distance (ft.)	26.37	25.84
Longitudinal #3 Distance (ft.)	30.87	30.34
Longitudinal #4 Distance (ft.)	35.37	34.84

The optimum cooling system would have the fiber optic laser transmitter and laser reciever at the pickup and kicker tanks. This is also the most conservative assumption for the calculations in this paper, since the propagation velocity of a signal in optical fiber is 67% of the speed of light, whereas the propagation velocity in good coaxial cable is 88% of the speed of light. Therefore, the amount of delay per physical distance is calculated using the propagation velocity of optical fiber.

Table 4.5: Calculation of the signal delay in optical fiber.

Parameter	Value
Speed of Light in Vacuum (m/ns)	0.299792458
Feet per Meter Conversion	3.280839895
Signal Speed in Fiber Optics (c)	67%
Nanoseconds per Foot in Fiber	1.52

There are other delays in a stochastic cooling system. The laser transmitter and reciever each have a delay associated with them. Similarly, amplifiers, attenuators, switches, and delay trombones all have delays associated with them. Finally, it takes time for the signal generated on the pickup electrode (and the kicker signal delivered to the kicker electrodes) to get to (come from) the electrical port on the vacuum tank. Standard numbers quoted by Ralph Pasquinelli for each of these sources of delay are listed in table 4.6.

Table 4.6: Miscellaneous delays in a standard stochastic cooling system.

Stochastic Cooling Component	Delay (ns)
Pickup Tank from Arrays to Port	5
Pickup Amplifiers and Trombones	5
Laser Transmittter	15
Miscellaneous Connecting Cables	15
Laser Link Reciever	15
Kicker Electronics	5
TWT	15
Kicker Tank from Port to Arrays	5
Total	80

Adding together all of the delays, the total signal delay for each stochasti cooling system is listed in table 4.7. Note that these numbers represent fairly conservative numbers and could be shortened by a number of techniques if required.

Table 4.7: Signal transmission delays in each of the 6 stochastic cooling systems for the Recycler ring. All delays are rounded up to the next integer number of nanoseconds.

Parameter	H	L1	L2	V	L3	L4
Miscellaneous Delays (ns)	80	80	80	80	80	80
Laser Telescope Delay (ns)	1685	1685	1685	1685	1685	1685
Vertical Fiber Chord Delay (ns)	40	40	40	40	40	40
Horizontal Fiber Chord Delay (ns)	174	174	174	174	174	174
Pickup to MIQ213 Delay (ns)	53	47	40	40	47	53
MIQ109 to Kicker Delay (ns)	117	47	40	40	47	53
SubTotal	2149	2073	2059	2059	2073	2085
Beam Path Delay (ns) [from T.3.2]	2082	1972	1972	1972	1972	1972
Net Delay	67	101	87	87	101	113

5. Signal Transmission Geometry: Cutting Corners

Because we need to decrease the delay in the signal transmission, the first method for reducing delays without compromising performance is to invoke more civil construction. The first change is to make the conduit between the laser telescope and the tunnel to a straight inclined tube.

Table 5.1: Signal transmission distances in the fiber optic cables of each of the 6 stochastic cooling systems for the Recycler ring.

Parameter	H	L1	L2	V	L3	L4
Transmission Across Tunnel (ft.)	20	20	20	20	20	20
Transmission Across Cave (ft.)	18	18	18	18	18	18
Length of Pickup Conduits (ft.)	70.2	70.2	70.2	33.0	33.0	33.0
Length of Kicker Conduits (ft.)	113.0	33.7	33.7	70.2	70.2	70.2
Length along Pickup Beamline (ft.)	4.5	0	4.5	4.5	0	4.5
Length along Kicker Beamline (ft.)	0	2.3	2.3	4.5	0	4.5
Total	225.7	144.2	148.7	150.2	141.2	150.2

The other change is to leave the path of the chord between the chord and tunnel and have direct conduits to each half cell, thereby eliminating the majority of the transmission line delay along the beamline. Figures 5.1 and 5.2 contain sketches of the new geometry.

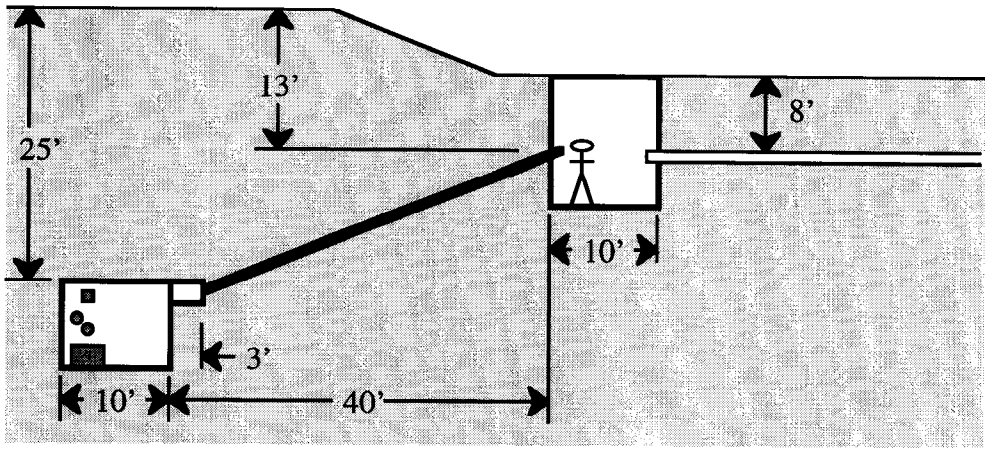

Figure 5.1: Elevation view along the chord between MIQ213 and MIQ109. In order to reduce the path length, the conduit between the laser telescope cave and the tunnel is a straight line.

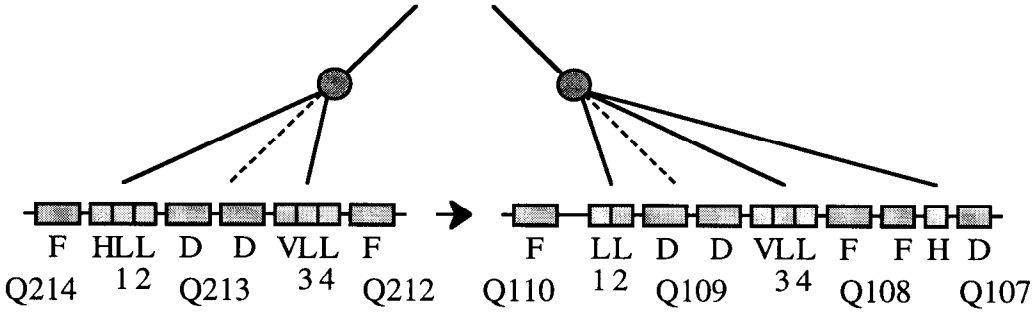

Figure 5.2: Plan view of the proposed conduit configuration between the laser telescope caves and the Recycler tunnel.

The new path lengths are listed in table 5.1. The final tally is summarized in table 5.2. The bottom line is that though the geometry change is helpful, it is not sufficient. More steps will be needed before a workable solution is found.

Table 5.2: Signal transmission delays in each of the 6 stochastic cooling systems for the Recycler ring. All delays are rounded up to the next integer number of nanoseconds.

Parameter	H	L1	L2	V	L3	L4
Miscellaneous Delays (ns)	80	80	80	80	80	80
Laser Telescope Delay (ns)	1685	1685	1685	1685	1685	1685
Fiber Optic Delay (ns)	343	220	226	229	215	229
SubTotal	2108	1985	1991	1994	1980	1994
Beam Path Delay (ns) [from T.3.2]	2082	1972	1972	1972	1972	1972
Net Delay	26	13	19	22	8	22

6. Signal Transmission Geometry: Shorter Optical Fibers

Using the same geometry as described in section 5, the change proposed in this section is to move the laser transmitters and recievers into the mini-alcoves bored into the side of the tunnel in order to hide these electronic elements 2' to 3' deep from radiation showers. Because the propagation speed of a signal is faster in a coaxial cable than in an optical fiber, this change has the effect of shortening the signal delay. The delays are summarized in table 6.1. The delay per distance in coaxial cable is 1.16 ns/ft.

Table 6.1: Signal transmission delays in each of the 6 stochastic cooling systems for the Recycler ring. All delays are rounded up to the next integer number of nanoseconds.

Parameter	H	L1	L2	V	L3	L4
Miscellaneous Delays (ns)	80	80	80	80	80	80
Laser Telescope Delay (ns)	1685	1685	1685	1685	1685	1685
Coaxial Cable Delay in Tunnel (ns)	29	26	31	34	24	34
Fiber Optic Delay (ns)	306	186	186	185	185	185
SubTotal	2100	1977	1982	1984	1974	1984
Beam Path Delay (ns) [from T.3.2]	2082	1972	1972	1972	1972	1972
Net Delay	18	5	10	12	2	12

7. Signal Transmission Geometry: No Optical Fibers

In this scenario the optical fibers are only in the cave just before launching the modulated laser signal into the telescope. Again, because the propagation speed of a signal is faster in a coaxial cable than in an optical fiber, this change has the effect of shortening the signal delay. The delays are listed in table 7.1. In this case there is no shortage of contingency in the signal delay across the chord.

Table 7.1: Signal transmission delays in each of the 6 stochastic cooling systems for the Recycler ring. All delays are rounded up to the next integer number of nanoseconds.

Parameter	H	L1	L2	V	L3	L4
Miscellaneous Delays (ns)	80	80	80	80	80	80
Laser Telescope Delay (ns)	1685	1685	1685	1685	1685	1685
Coaxial Cable Delay (ns)	262	168	173	175	164	175
SubTotal	2027	1933	1938	1940	1929	1940
Beam Path Delay (ns) [from T.3.2]	2082	1972	1972	1972	1972	1972
Net Delay	-55	-39	-34	-32	-43	-32

8. Signal Transmission Geometry: No Optical Fibers & Original Geometry

Because the case in section 7 was so favorable, it is worthwhile to ask if the simpler civil construction geometry is sufficient when no optical fiber transmission is assumed. The delays are listed in table 8.1. It is obvious that the geometry and signal transmission method in section 7 is required since the geometry simplification attempted here yielded insufficient signal delay savings.

Table 8.1: Signal transmission delays in each of the 6 stochastic cooling systems for the Recycler ring. All delays are rounded up to the next integer number of nanoseconds.

Parameter	H	L1	L2	V	L3	L4
Miscellaneous Delays (ns)	80	80	80	80	80	80
Laser Telescope Delay (ns)	1685	1685	1685	1685	1685	1685
Vertical Coaxial Cable Delay (ns)	31	31	31	31	31	31
Horz. Coaxial Cable Delay (ns)	133	133	133	133	133	133
Pickup to MIQ213 Delay (ns)	41	36	30	31	36	41
MIQ109 to Kicker Delay (ns)	90	36	31	30	34	41
SubTotal	2060	2001	1990	1990	1999	2011
Beam Path Delay (ns) [from T.3.2]	2082	1972	1972	1972	1972	1972
Net Delay	-22	29	18	18	27	39